Advanced hydrogenation process applied on Ge on Si quantum dots for enhanced light emission

Lukas Spindlberger, Moonyong Kim, Johannes Aberl, Thomas Fromherz, Friedrich Schäffler, Frank Fournel, Jean-Michel Hartmann, Brett Hallam, Moritz Brehm

RESEARCH ARTICLE | FEBRUARY 23 2021

Advanced hydrogenation process applied on Ge on Si quantum dots for enhanced light emission

Lukas Spindlberger ; Moonyong Kim ; Johannes Aberl; Thomas Fromherz ; Friedrich Schäffler; Frank Fournel; Jean-Michel Hartmann; Brett Hallam ; Moritz Brehm

Appl. Phys. Lett. 118, 083104 (2021)
https://doi.org/10.1063/5.0036039

Applied Physics Letters ARTICLE scitation.org/journal/apl

Advanced hydrogenation process applied on Ge on Si quantum dots for enhanced light emission

Cite as: Appl. Phys. Lett. **118**, 083104 (2021); doi: 10.1063/5.0036039
Submitted: 2 November 2020 · Accepted: 6 February 2021 ·
Published Online: 23 February 2021

Lukas Spindlberger,[1,a)] Moonyong Kim,[2] Johannes Aberl,[1] Thomas Fromherz,[1] Friedrich Schäffler,[1] Frank Fournel,[3] Jean-Michel Hartmann,[3] Brett Hallam,[2] and Moritz Brehm[1]

AFFILIATIONS

[1]Institute of Semiconductor and Solid State Physics, Johannes Kepler University Linz, Altenberger Strasse 69, 4040 Linz, Austria
[2]School of Photovoltaic and Renewable Energy Engineering, The University of New South Wales, Kensington, NSW 2052, Australia
[3]Université Grenoble Alpes, CEA, LETI, 38054 Grenoble, France

[a)]Author to whom correspondence should be addressed: lukas.spindlberger@jku.at

ABSTRACT

For the development of photonic integrated circuits, it is mandatory to implement light sources on a Si-on-insulator (SOI) platform. However, point defects in the Si matrix and, e.g., at the Si/SiO_2 interface act as nonradiative recombination channels, drastically limiting the performance of Si-based light emitters. In this Letter, we study how these defects can be healed by applying an advanced hydrogenation process, recently developed in photovoltaic research for the passivation of performance-limiting defects in Si solar cells. Upon hydrogenation, we observe an increase in the room temperature photoluminescence (PL) yield by a factor of more than three for defect-enhanced quantum dots (DEQDs) grown on float-zone Si substrates, revealing the potential of this technique to passivate detrimental defects. For DEQDs grown using SOI substrates, the PL yield enhancement even exceeds a factor of four, which we attribute to the additional passivation of defects originating from the substrate. The results for SOI substrates are of particular interest due to their relevance for future photonic integrated circuits.

The passivation of dangling bonds (DBs) in Si and at the Si/SiO_2 interface with hydrogen is crucial for the performance of optoelectronic devices, where DBs act as nonradiative recombination centers that limit the charge carrier lifetimes.[1–4] Over the last couple of years, the photovoltaic industry has triggered substantial research efforts toward the passivation of defects like the boron-oxide (B–O) complex, rare earth impurities, and DB defects. In this context, recently developed hydrogenation processes proved to be highly effective for the passivation of these detrimental defects which enabled the use of more cost-effective multi-crystalline Si substrates for solar cells.[5–8]

Similarly, full control over detrimental defects[9] will turn out to be crucial for future Si-based optoelectronics to reach its maximum potential.[10,11] This is also true for a recently discovered light-emitting system, the so-called defect-enhanced quantum dot (DEQD). Present knowledge indicates that by *in situ* implantation of Ge ions during growth, beneficial self-interstitial defects are created within the Ge QDs.[12–14] Their enhanced room temperature (RT) light emission suggests that strong modifications of the electronic states are caused by these self-interstitial defects.[13–15] Electrons that are excited in the Si-matrix can tunnel to the defect-induced states and recombine with holes that are confined in the QD by the large band offsets between Ge and Si. Defect-enhanced quantum dots have already been used as gain material in optically pumped lasers[12–14] and also in light-emitting diodes up to RT and beyond.[16]

However, for the use of DEQDs in photonic integrated circuits (PICs), it is essential to transfer the DEQD growth-concept from a bulk Si to a Si-on-insulator (SOI) platform. Although SOI substrates are advantageous for the fabrication of active or passive photonic components for PICs,[17] the growth on SOI gives rise to several challenges. The much lower thermal conductivity of the thick buried oxide (BOX) layer compared to float-zone-Si (FZ-Si) bulk could reduce the available thermal budget for annealing processes. Due to the SOI fabrication procedure,[18] additional defects can occur, e.g., between the Si device layer and the BOX layer which are detrimental for charge carrier lifetimes and radiative recombinations.[19,20]

In this Letter, we demonstrate that an advanced hydrogenation process (AHP),[5–8,21,22] developed for the silicon photovoltaic industry, can also be applied on DEQDs without further adaptation to passivate lifetime-killing defects in the Si matrix that ultimately limit the photoluminescence (PL) yield. Thereby, the AHP process does not

negatively affect the self-interstitials within the Ge QDs required for efficient light emission. Thus, while the spectral shape of DEQD emission remains unaffected, the passivation leads to significant PL enhancement by a factor of more than three.

DEQDs were grown on high-resistivity (>1000 Ω cm) FZ-Si(001) substrates using a Riber Siva 45 solid-source molecular beam epitaxy chamber. After RCA cleaning of the sample,[23] the native Si oxide was removed using a dip in diluted (1%) hydrofluoric acid (HF) right before the samples were introduced into the load-lock chamber. The cleaning procedure is concluded by an *in situ* degassing step at 720 °C for 30 min. 50 nm thick Si buffer layers were grown at growth temperatures T_G ramped from 550 °C to 500 °C with a rate of 0.95 Å s^{-1}. Subsequently, Ge with a nominal thickness of $\theta_{Ge} = 8.4$ Å was deposited at $T_G = 500$ °C. Ge QDs nucleate via the Stranski–Krastanow growth mode,[24] where a Ge-rich two-dimensional wetting layer is formed first, followed by strain-driven QD formation,[12,25–31] which evolve in the shape of hut clusters under the applied growth conditions.[32] During Ge deposition, the sample was *in situ* implanted with Ge^+ ions [Fig. 1(a)] by applying a voltage of −2 kV between the Ge source and the substrate holder. The concentration of Ge^+ ions implanted this way is approximately 10^{12} ions cm^{-2}.[12–14] Finally, the QDs were capped with 70 nm of Si [Fig. 1(b)], deposited at a T_G ramped up from 475 °C to 570 °C during the Si deposition process.

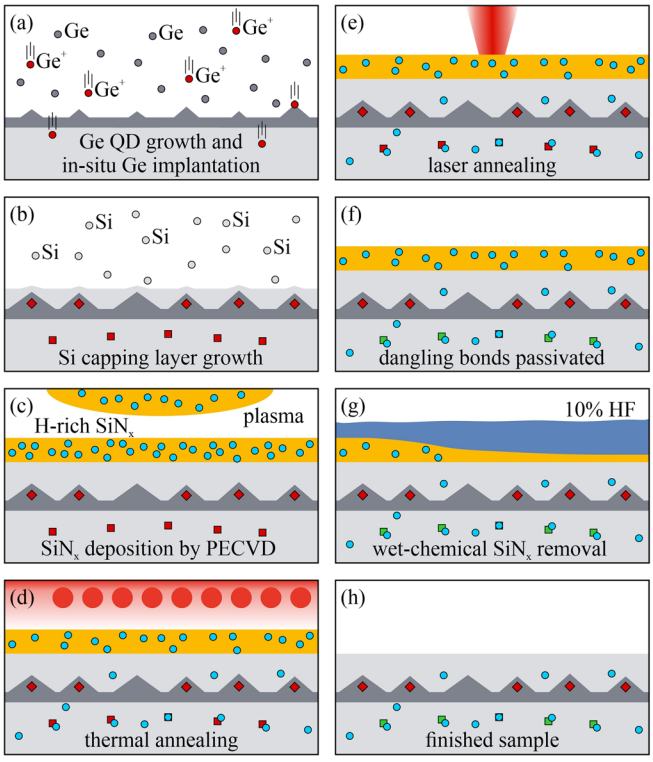

FIG. 1. Sketch of the fabrication and hydrogenation process. (a) Growth of DEQDs by molecular beam epitaxy. Ge^+ ions marked as red spheres are implanted into the Ge QDs. (b) Growth of the Si capping layer. Defects in the Si matrix and in the Ge QDs are marked by red squares and diamonds, respectively. (c) Deposition of 75 nm of H-rich SiN_x by PECVD. Hydrogen atoms are marked as blue spheres. (d) Hydrogen is driven into the Si matrix by the firing step (740 °C) in a belt furnace. (e) Laser annealing. (f) Passivated dangling bonds in Si marked as green squares. The interstitials within the Ge DEQDs remain unaffected by the hydrogen treatment.[34] (g) The SiN_x layer is removed using 10% HF. (h) Finished sample.

Furthermore, a single layer and a multilayer DEQD sample were grown on a SOI substrate specifically elaborated from a commercial SOI wafer in order to have a specific 2 μm thick BOX layer beneath a 70 nm thick intrinsic Si device layer.[18] The very same cleaning procedure was applied to the SOI substrates before growth. Si buffer layers with 80 nm and 30 nm thickness were grown at growth temperatures T_G ramped from 550 °C to 500 °C with a rate of 0.9 Å s^{-1} for the single layer and multilayer sample, respectively. For each DEQD layer, $\theta_{Ge} = 7.5$ Å of Ge was deposited at $T_G = 500$ °C while applying −1.5 kV to the substrate, followed by the deposition of a 16 nm thick Si spacer layer grown at T_G ramped from 475 °C to 600 °C. The single DEQD layer was capped with 55 nm of Si at $T_G = 500$ °C before sample annealing at 575 °C for 30 min. For the multilayer, the growth was concluded after seven DEQD-layers by the deposition of 5 nm of Si at $T_G = 500$ °C and subsequent annealing at 575 °C for 60 min.

The samples were treated using hydrogen passivation as described in detail in Refs. 5–8, 21, and 22. This consisted of a RCA cleaning and the deposition of a 75 nm thick layer of H-rich silicon nitride (SiN_x) at $T = 400$ °C by plasma-enhanced chemical vapor deposition (PECVD), see Fig. 1(c).[33] Other passivation techniques, such as sample annealing in H_2N_2 atmosphere could in principle be employed as well. However, the hydrogen supply from the SiN_x layer can have another benefit in electrically driven devices based on DEQDs, where isolating layers are needed anyway. Thermal annealing (firing) was done in an inline Schmid metallization fast-firing belt furnace [Fig. 1(d)] at 740 °C±6 °C (as measured on standard 200 μm thick silicon wafers), with a constant belt speed of 177 in. per minute, which corresponds to an annealing time of about three seconds. For laser annealing, the samples were illuminated with a 938 nm fiber-coupled laser diode [Fig. 1(e)] with a photon flux exceeding 2.94×10^{19} cm^{-2} s^{-1} for 10 s, while the temperature of the sample was kept at approximately 300 °C. The laser was operated in quasi-continuous mode with a repetition rate of 2 kHz and pulse length of 0.5 ms.[5] The deposited SiN_x has a refractive index of ∼2.08 at a wavelength of 633.2 nm and, thus, acts as an antireflection coating for visible light. Therefore, the SiN_x layer was wet-chemically removed prior to PL measurements using 10% HF [Fig. 1(g) and supplementary material]. For the PL measurements at 10 K, the samples were mounted into a continuous helium flow cryostat equipped with a heatable cold finger, allowing for sample temperatures between 4 K and 350 K. A fiber-coupled continuous-wave diode laser emitting at 442 nm was used for excitation. An objective with a numerical aperture of 0.7 focused the laser on the sample's surface, resulting in a laser spot size of ∼3 μm and an intensity of ∼32 kW cm^{-2}. The near-infrared PL signal was collected by the very same objective and routed via a multimode fiber to a 300 mm grating spectrometer equipped with a 300 gr/mm grating. Two liquid nitrogen-cooled InGaAs photodiode arrays (OMA V by Princeton Instruments with 512 and 1024 pixels) with a cutoff wavelength of 1580 nm were used for detection. To be able to compare the spectra recorded with the two different detectors, an untreated DEQD reference sample was included in every measurement. Thus, we were able to adapt the scaling of the spectra to different collection and detection efficiencies by normalization via the PL intensity of the common reference.

To exclude changes in the spectral shape upon excessive thermal annealing-induced Si–Ge intermixing of the DEQDs, as reported previously,[35] we first isolate the influence of the firing and the laser annealing steps on the RT PL. Figure 2 shows the RT PL signal of DEQDs grown on FZ-Si before and after the firing process [Fig. 2(a)], laser annealing [Fig. 2(b)], and the combination of both [Fig. 2(c)]. Note that for the different annealing processes, no changes in the spectral shape of the PL emission are present, while a small but distinct increase in the PL yield of up to 36% is observed, comparable to results with millisecond flash lamp annealing.[36]

In a second step, the influence of the AHP was studied. In Fig. 3(a), the corresponding RT PL spectra are shown before and after the hydrogenation process, albeit without laser annealing. An increase in the integrated PL intensity of almost a factor of three is observed. Figure 3(b) reveals the RT PL before and after the whole AHP, i.e., including the laser annealing step. Here, the integrated intensity increases by more than a factor of three. Further experiments on samples with slightly different annealing parameters indicate that the PL increase is fairly robust against the exact annealing conditions (not shown). The preservation of the spectral shape of the DEQD PL along with the multifold enhanced light emission of both, Si bulk and the DEQDs, indicate that the AHP effectively passivates defects in the Si matrix that else lead to nonradiative recombination.

In earlier works, an increase in the RT PL emission of DEQDs was also observed after low-energy proton irradiation.[35] However, this approach leads to the formation of G-centers, creating additional recombination paths at cryogenic temperatures, observable by a spectral feature at 1279 nm.[37] Because these G-centers are typically formed by an ion-irradiation process, they are not expected to be present in the low temperature spectra in this work. This assumption is confirmed by the PL spectra recorded at 10 K [Figs. 3(c) and 3(d)]. As compared to RT a narrowing and a slight red-shift of the DEQD-related emission is observed. Furthermore, no additional defect-related features are detected.

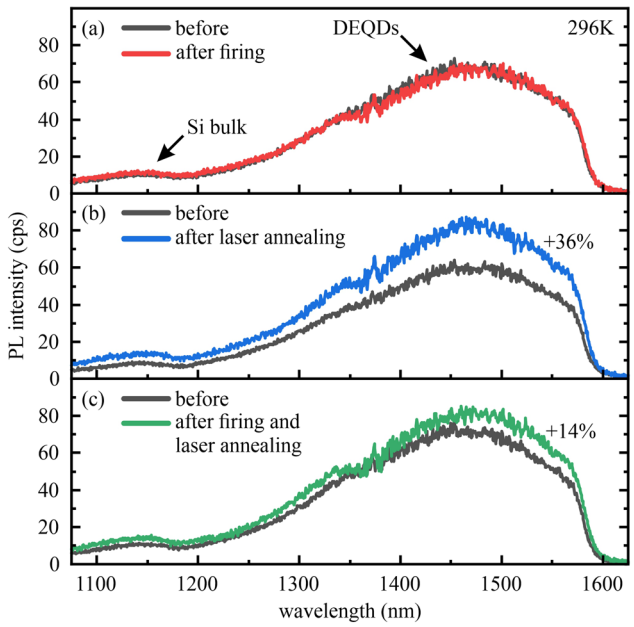

FIG. 2. PL spectra recorded at RT before and after (a) firing, (b) laser annealing, (c) firing and subsequent laser annealing.

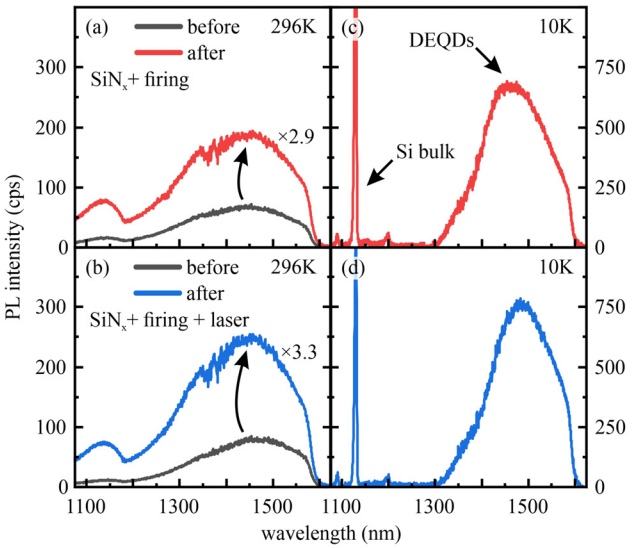

FIG. 3. (a) and (b) PL spectra recorded at RT before and after the AHP including SiN_x deposition and subsequent annealing. (c) and (d) PL spectra recorded at 10 K of the samples after hydrogenation.

The RT PL spectra before and after the AHP of a single DEQD layer and of a sevenfold multilayer both grown on SOI substrates are shown in Figs. 4(a) and 4(b), respectively. The slightly higher temperatures during the Si overgrowth of the DEQDs and the subsequent *in situ* annealing at 575 °C led to enhanced intermixing of the Ge

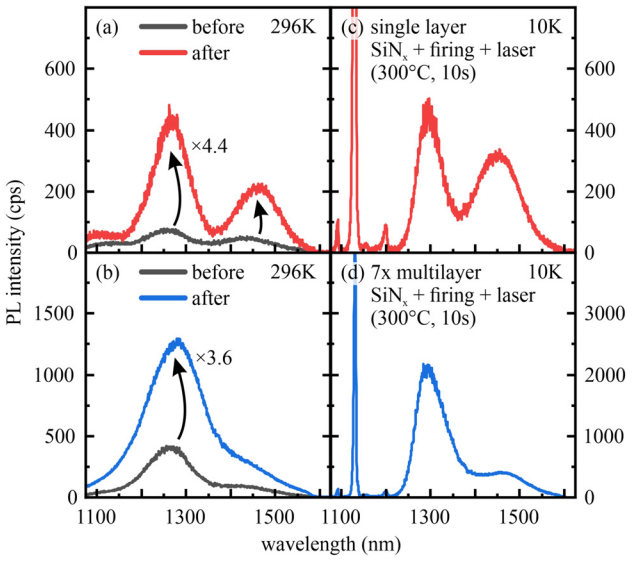

FIG. 4. (a) and (b) PL spectra recorded at RT of a single layer and a 7× multilayer grown on SOI substrates before and after the AHP. PL spectra after the AHP recorded at 10 K of (c) a DEQD single layer and (d) of a DEQD 7× multilayer.

DEQDs with the surrounding Si matrix. Thus, the PL emission shifts to higher energies as compared to the samples grown on FZ-Si (Fig. 3), enabling to additionally cover the telecom O-band around 1300 nm. In the emission spectra of the DEQDs grown on SOI substrates (Fig. 4), pronounced dips are observed around 1365 nm. As shown in Figs. 2 and 3, similar dips are absent in the spectra of DEQDs grown on bulk substrates. We ascribe these emission minima to the electric field mode's shape, propagating perpendicular to the substrate's surface in the outward direction. For DEQD layers on SOI substrates, this mode profile is strongly modulated in the region of the BOX and DEQD layers due to the interference of electric field components reflected at the BOX layer's interfaces. At 1365 nm, a mode profile minimum coincides with the DEQD position, resulting in a reduced intensity of the vacuum field fluctuations and, thus, in a reduced spontaneous DEQD emission rate at this wavelength.[38] This assignment is based on the measurement and simulation of the sample's reflection spectra, showing distinct Fabry–Pérot fringes dominated by the 2 μm thick BOX layer of the SOI substrate. It is further confirmed by RT PL experiments at various sample inclinations with respect to the optical axis of the PL setup. In these experiments, the emission minimum systematically shifts toward shorter wavelength with increasing inclination angle, clearly indicating an interference effect as opposed to an inherent property of the DEQD electronic energy level structure. For the samples containing seven DEQD layers on a SOI substrate, the spectra shown in Figs. 4(b) and 4(d) show less pronounced dips since the DEQD layers are distributed in growth direction over approximately 100 nm and consequently smear out the mode minimum.

As for the bulk Si substrates, application of the AHP leads for the DEQDs grown on SOI to a tremendous increase in the integrated RT PL by a factor of 4.4× for the single layer and 3.6× for the multilayer sample. We attribute the higher relative PL increase compared to the samples on FZ-Si to the additional passivation of point defects originating from the SOI fabrication procedure. The PL spectra recorded at 10 K are shown in Figs. 4(c) and 4(d). No additional luminescence features from potential defects at the BOX layer/Si device layer interface were observed.[20]

In this Letter, we have shown that the light-emitting performance of DEQDs can be significantly increased by applying an advanced hydrogenation process, recently developed in photovoltaic research for curing performance limiting defects in Si solar cells. Supplying hydrogen from a hydrogen-rich SiN_x layer in combination with thermal annealing processes increases the PL yield of DEQDs grown on bulk Si substrates by about a factor of three. As compared to other hydrogen-related treatments like low-energy proton irradiation,[35] the approach presented in this work has the advantage of not promoting further unintentional radiative recombination paths.

For future applications, e.g., in photonic integrated circuits, however, the growth of DEQDs on SOI substrates is of major interest. We demonstrated that the low thermal conductivity of the BOX layer and hence the reduced thermal budget pose no limitation on the use of DEQDs on SOI within industry graded thermal processes like firing at 740 °C±6 °C for several seconds and laser annealing at 300 °C for several seconds. Additionally, the emission enhancement for DEQDs grown on SOI is more pronounced (exceeding a factor of four) than for the FZ-Si samples. Since the epitaxial growth procedure was very similar, we attribute this to the passivation of additional defects originating from the SOI fabrication procedure.

While the SiN_x layer acts in solar cells simultaneously as hydrogen source and as antireflection coating, it could be easily implemented in the fabrication processes of other Si-based devices, like light emitting diodes, without additional fabrication steps. The SiN_x could be used as a sidewall passivation layer to reduce leakage currents and simultaneously act as hydrogen source. The hydrogen is expected to not only passivate defects as described in this Letter, but also ionized donors and acceptors in the highly doped regions of optoelectronic devices, resulting in further performance improvement. Note that the advanced hydrogenation process is not limited to light-emitting devices, but could also be beneficial for other active components in PICs or nanoelectronic devices known to be sensitive to point defects.

See the supplementary material for the influence of hydrofluoric acid etching on the Si surface roughness and the PL yield.

This work was funded by the Austrian Science Fund (FWF): Nos. Y1238-N36 and P30564-NBL and the Linz Institute of Technology (LIT): No. LIT-2019-7-SEE-114. Funding was also provided by the EU H2020 QuantERA ERA-NET via the Quantum Technologies project CUSPIDOR, which is co-funded by FWF(I3760).

DATA AVAILABILITY

The data that support the findings of this study are available from the corresponding author upon reasonable request.

REFERENCES

[1]E. Cartier, J. H. Stathis, and D. A. Buchanan, Appl. Phys. Lett. **63**, 1510 (1993).
[2]S. Castellanos, K. E. Ekstrøm, A. Autruffe, M. A. Jensen, A. E. Morishige, J. Hofstetter, P. Yen, B. Lai, G. Stokkan, C. del Cãizo, and T. Buonassisi, IEEE J. Photovoltaics **6**, 632 (2016).
[3]S. Steffens, C. Becker, D. Amkreutz, A. Klossek, M. Kittler, Y.-Y. Chen, A. Schnegg, M. Klingsporn, D. Abou-Ras, K. Lips, and B. Rech, Appl. Phys. Lett. **105**, 022108 (2014).
[4]T. Taishi, T. Hoshikawa, M. Yamatani, K. Shirasawa, X. Huang, S. Uda, and K. Hoshikawa, J. Cryst. Growth **306**, 452 (2007).
[5]B. J. Hallam, P. G. Hamer, S. Wang, L. Song, N. Nampalli, M. D. Abbott, C. E. Chan, D. Lu, A. M. Wenham, L. Mai, N. Borojevic, A. Li, D. Chen, M. Y. Kim, A. Azmi, and S. Wenham, Energy Procedia **77**, 799 (2015).
[6]M. Kim, D. Chen, M. Abbott, S. Wenham, and B. Hallam, AIP Conf. Proc. **1999**, 130010 (2018).
[7]B. J. Hallam, P. G. Hamer, S. R. Wenham, M. D. Abbott, A. Sugianto, A. M. Wenham, C. E. Chan, G. Xu, J. Kraiem, J. Degoulange, and R. Einhaus, IEEE J. Photovoltaics **4**, 88 (2014).
[8]B. Hallam, D. Chen, M. Kim, B. Stefani, B. Hoex, M. Abbott, and S. Wenham, Phys. Status Solidi A **214**, 1700305 (2017).
[9]D. Hiller, V. P. Markevich, J. A. T. de Guzman, D. König, S. Prucnal, W. Bock, J. Julin, A. R. Peaker, D. Macdonald, N. E. Grant, and J. D. Murphy, Phys. Status Solidi A **217**, 2000436 (2020).
[10]K. Makihara, S. Fujimori, M. Ikeda, A. Ohta, and S. Miyazaki, Mater. Sci. Semicond. Process. **120**, 105250 (2020).
[11]B. Julsgaard, N. von den Driesch, P. Tidemand-Lichtenberg, C. Pedersen, Z. Ikonic, and D. Buca, Photonics Res. **8**, 788 (2020).
[12]M. Brehm and M. Grydlik, Nanotechnology **28**, 392001 (2017).
[13]M. Grydlik, F. Hackl, H. Groiss, M. Glaser, A. Halilovic, T. Fromherz, W. Jantsch, F. Schäffler, and M. Brehm, ACS Photonics **3**, 298 (2016).
[14]M. Grydlik, M. T. Lusk, F. Hackl, A. Polimeni, T. Fromherz, W. Jantsch, F. Schäffler, and M. Brehm, Nano Lett. **16**, 6802 (2016).
[15]F. Murphy-Armando, M. Brehm, P. Steindl, M. T. Lusk, T. Fromherz, K. Schwarz, and P. Blaha, "Light-emission from direct bandgap Germanium containing split-interstitial defects," Phys. Rev. B (to be published).

[16]P. Rauter, L. Spindlberger, F. Schäffler, T. Fromherz, J. Freund, and M. Brehm, ACS Photonics **5**, 431 (2018).
[17]V. Stojanović, R. J. Ram, M. Popović, S. Lin, S. Moazeni, M. Wade, C. Sun, L. Alloatti, A. Atabaki, F. Pavanello, and P. Bhargava, Opt. Express **26**, 13106 (2018).
[18]H. Moriceau, F. Rieutord, F. Fournel, Y. L. Tiec, L. D. Cioccio, C. Morales, A. M. Charvet, and C. Deguet, Adv. Nat. Sci. **1**, 043004 (2011).
[19]*Silicon, Germanium, and Their Alloys: Growth, Defects, Impurities, and Nanocrystals*, edited by G. Kissinger and S. Pizzini (CRC Press, 2014).
[20]N. Hauke, A. Tandaechanurat, T. Zabel, T. Reichert, H. Takagi, M. Kaniber, S. Iwamoto, D. Bougeard, J. J. Finley, G. Abstreiter, and Y. Arakawa, New J. Phys. **14**, 083035 (2012).
[21]A. G. Aberle, Sol. Energy Mater. Sol. Cells **65**, 239 (2001).
[22]A. Herguth, G. Schubert, M. Kaes, and G. Hahn, Prog. Photovoltaics **16**, 135 (2008).
[23]W. Kern, J. Electrochem. Soc. **137**, 1887 (1990).
[24]I. N. Stranski and L. V. Krastanow, Sitzungsber. Akad. Wiss. Wien, Math.-Naturwiss. Kl., Abt. 2B **146**, 797 (1938).
[25]G. Capellini, M. D. Seta, and F. Evangelisti, Appl. Phys. Lett. **78**, 303 (2001).
[26]I. Berbezier and A. Ronda, Surf. Sci. Rep. **64**, 47 (2009).
[27]C. Dais, G. Mussler, H. Sigg, E. Müller, H. H. Solak, and D. Grützmacher, J. Appl. Phys. **105**, 122405 (2009).
[28]L. Persichetti, A. Sgarlata, M. Fanfoni, and A. Balzarotti, J. Phys. **27**, 253001 (2015).
[29]J. Zhang, M. Brehm, M. Grydlik, and O. G. Schmidt, Chem. Soc. Rev. **44**, 26 (2015).
[30]M. V. Shaleev, A. V. Novikov, N. A. Baydakova, A. N. Yablonskiy, O. A. Kuznetsov, D. N. Lobanov, and Z. F. Krasilnik, Semiconductors **45**, 198 (2011).
[31]H. Groiss, L. Spindlberger, P. Oberhumer, F. Schäffler, T. Fromherz, M. Grydlik, and M. Brehm, Semicond. Sci. Technol. **32**, 02LT01 (2017).
[32]Y.-W. Mo, D. E. Savage, B. S. Swartzentruber, and M. G. Lagally, Phys. Rev. Lett. **65**, 1020 (1990).
[33]Z. Hameiri, N. Borojevic, L. Mai, N. Nandakumar, K. Kim, and S. Winderbaum, IEEE J. Photovoltaics **7**, 996 (2017).
[34]J. R. Weber, A. Janotti, and C. G. Van de Walle, Phys. Rev. B **87**, 035203 (2013).
[35]L. Spindlberger, J. Aberl, A. Polimeni, J. Schuster, J. Hörschläger, T. Truglas, H. Groiss, F. Schäffler, T. Fromherz, and M. Brehm, Crystals **10**, 351 (2020).
[36]L. Spindlberger, S. Prucnal, J. Aberl, and M. Brehm, Phys. Status Solidi A **216**, 1900307 (2019).
[37]C. Beaufils, W. Redjem, E. Rousseau, V. Jacques, A. Y. Kuznetsov, C. Raynaud, C. Voisin, A. Benali, T. Herzig, S. Pezzagna, J. Meijer, M. Abbarchi, and G. Cassabois, Phys. Rev. B **97**, 035303 (2018).
[38]C. Creatore and L. C. Andreani, Phys. Rev. A **78**, 063825 (2008).